



**HAL**  
open science

## Order statistics and heavy-tail distributions for planetary perturbations on Oort cloud comets

Radu S. Stoica, Shuyan Liu, Youri Davydov, Marc Fouchard, Alain Vienne,  
Giovanni Valsecchi

► **To cite this version:**

Radu S. Stoica, Shuyan Liu, Youri Davydov, Marc Fouchard, Alain Vienne, et al.. Order statistics and heavy-tail distributions for planetary perturbations on Oort cloud comets. *Astronomy & Astrophysics* - A&A, 2010, 513 (A14), 9 p. 10.1051/0004-6361/200912871 . hal-00519715

**HAL Id: hal-00519715**

**<https://hal.science/hal-00519715v1>**

Submitted on 4 Apr 2022

**HAL** is a multi-disciplinary open access archive for the deposit and dissemination of scientific research documents, whether they are published or not. The documents may come from teaching and research institutions in France or abroad, or from public or private research centers.

L'archive ouverte pluridisciplinaire **HAL**, est destinée au dépôt et à la diffusion de documents scientifiques de niveau recherche, publiés ou non, émanant des établissements d'enseignement et de recherche français ou étrangers, des laboratoires publics ou privés.



Distributed under a Creative Commons Attribution 4.0 International License

# Order statistics and heavy-tailed distributions for planetary perturbations on Oort cloud comets

R. S. Stoica<sup>1</sup>, S. Liu<sup>1</sup>, Yu. Davydov<sup>1</sup>, M. Fouchard<sup>2,3,\*</sup>, A. Vienne<sup>2,3</sup>, and G. B. Valsecchi<sup>4</sup>

<sup>1</sup> University Lille 1, Laboratoire Paul Painlevé, 59655 Villeneuve d'Ascq Cedex, France

<sup>2</sup> University Lille 1, LAL, 59000 Lille, France  
e-mail: marc.fouchard@univ-lille1.fr

<sup>3</sup> Institut de Mécanique Céleste et Calcul d'Ephémérides, 77 av. Denfert-Rochereau, 75014 Paris, France

<sup>4</sup> INAF – IASF, via Fosso del Cavaliere 100, 00133 Roma, Italy

Received 12 July 2009 / Accepted 19 November 2009

## ABSTRACT

**Aims.** This paper tackles important aspects of comet dynamics from a statistical point of view. Existing methodology uses numerical integration to compute planetary perturbations to simulate such dynamics. This operation is highly computational. It is reasonable to investigate a way in which a statistical simulation of the perturbations can be handled more easily.

**Methods.** The first step to answer such a question is to provide a statistical study of these perturbations in order to determine their main features. The statistical tools used are order statistics and heavy-tailed distributions.

**Results.** The study carried out indicated a general pattern exhibited by the perturbations around the orbits of the planets. These characteristics were validated through statistical testing and a theoretical study based on the Öpik theory.

**Key words.** methods: statistical – celestial mechanics – Oort Cloud

## 1. Introduction

Comet dynamics are among the most difficult phenomena to model in celestial mechanics. Indeed their dynamics is strongly chaotic, which makes individual motions of known comets hardly reproducible for more than a few orbital periods. When the origin of comets is under investigation, one has to fall back on the use of statistical tools in order to model the motion of a huge number of comets supposed to be representative of the actual population. Ideally, statistical modelling should also be reliable on a time scale comparable to the age of the solar system.

Due to their very elongated shapes, comet trajectories are affected by planetary perturbations during close encounters with planets. In particular, the perturbations induced by the major planets are fundamental in determining the evolution of comet trajectories. Consequently, it is of major importance to model these perturbations in a way which is statistically reliable and which needs the shortest computing time.

A direct numerical integration of a six-bodies-restricted problem (Sun, Jupiter, Saturn, Uranus, Neptune, Comet) for each time a comet enters the planetary region of the solar system is not possible due to the cost in computer time.

Looking for an alternative approach, we can take advantage of the fact that planetary perturbations for the Oort cloud comets are uncorrelated. In fact the orbital periods of such comets are so much longer than those of the planets that when the comet returns, the phases of the latter can be taken at random. Thus we can build a synthetic integrator à la Froeschlé and Rickman (Froeschlé & Rickman 1981) to speed up the modeling. The criticism by Fouchard et al. (2003) to such an approach does not

apply in the present case because, as was pointed out above, successive planetary perturbations of Oort cloud comets are uncorrelated.

The aim of this paper is to give a statistical description of a large set of planetary perturbations assumed to be representative of those acting on Oort cloud comets entering the planetary region. To this purpose we use order statistics and heavy-tailed distributions.

The rest of this paper is organised as follows. Section 2 is devoted to the presentation of the mechanism producing the data, i.e. the planetary perturbations and the statistical tools used to analyse the data. These tools are order statistics and heavy-tail distributions, which respectively allow the study and the modeling of the data distribution, with special attention to its symmetry, skewness and tail fatness. The obtained results are shown and interpreted in the third section. The results are finally analysed from a more theoretical point of view using the Öpik theory in Sect. 4. The paper closes with conclusions and perspectives.

## 2. Statistical tools

### 2.1. Data compilation

By planetary perturbations we mean the variations of the orbital parameters between their values before entering the planetary region of the solar system, i.e. the barycentric orbital element of the osculating cometary orbit  $(z_i, q_i, \cos i_i, \omega_i, \Omega_i)^T$  (where  $q$ ,  $i$ ,  $\omega$ ,  $\Omega$  are the perihelion distance, the inclination, the argument of perihelion and the longitude of the ascending node and  $z = -1/a$  with  $a$  the semi-major axis), and their final values  $(z_f, q_f, \cos i_f, \omega_f, \Omega_f)^T$  that is either when the comet is at its aphelion or when it is back on a Keplerian barycentric orbit.

\* Present address: observatoire de Lille, 1 Impasse de l'Observatoire, 59 000 Lille, France.

Between its initial and final values, the system Sun + Jupiter + Saturn + Uranus + Neptune + comet is integrated using the RADAU integrator at the 15th order (Everhart 1985) for a maximum of 2000 yrs. Then the planetary perturbations obtained through this integration are  $(\Delta z = z_f - z_i, \Delta q = q_f - q_i, \Delta \cos i = \cos i_f - \cos i_i, \Delta \omega = \omega_f - \omega_i, \Delta \Omega = \Omega_f - \Omega_i)^T$ . The details on the numerical experiment used to perform the integrations may be found in Rickman et al. (2001).

Repeating the above experiment with a huge number of comets (namely 9 600 000), one gets a set of planetary perturbations. The comets are chosen with uniform distribution of the perihelion distance between 0 and 32 AU, the cosine of the ecliptic inclination between  $-1$  and  $1$  and the argument of perihelion, and the longitude of the ascending node between 0 and  $360^\circ$ . The initial mean anomaly is chosen in a way that the perihelion passage on its initial Keplerian orbit occurs randomly with a uniform distribution between 500 and 1500 years after the beginning of the integration.

In the present study each perturbation is associated to the couple  $(\cos i_i, q_i)$  because the perturbations are mainly depending on  $q_i$  and  $\cos i_i$  (Fernández 1981). Similarly, since the orbital energy is the main quantity which is affected by the planetary perturbations, we will consider only these perturbations here.

Consequently, our data are composed by a set of triplets  $(\cos i_i, q_i, Z)$  where  $Z = z_f - z_i$  denotes the perturbations of the cometary orbital energy by the planets, and  $(\cos i_i, q_i)$  a point in a space denoted by  $K$ . We call  $Z$  the perturbation mark for the remainder of the paper.

## 2.2. Exploratory analysis based on order statistics

Let  $Z_1, \dots, Z_n$  be a sequence of independent identically distributed random variables and let  $F(z) = P(Z \leq z), z \in \mathbb{R}$  be the corresponding cumulative distribution function. Let us consider also  $\Sigma_n$ , the set of permutations on  $\{1, \dots, n\}$ .

The order statistics of the sample  $(Z_1, \dots, Z_n)$  is the rearrangement of the sample in increasing order and it is denoted by  $(Z_{(1,n)}, \dots, Z_{(n,n)})$ . Hence  $Z_{(1,n)} \leq \dots \leq Z_{(n,n)}$ , and there exists a random permutation  $\sigma_n \in \Sigma_n$  in the form of

$$(Z_{(1,n)}, \dots, Z_{(n,n)}) = (Z_{\sigma_n(1)}, \dots, Z_{\sigma_n(n)}). \quad (1)$$

Below some classical results from the literature are presented (David 1981; Delmas & Jourdain 2006). If  $F$  is continuous, then almost surely  $Z_{(1,n)} < \dots < Z_{(n,n)}$  and the permutation  $\sigma_n$  in definition (1) is unique. If  $Z_1$  has a probability density  $f$ , then the probability density of the order statistics is given by

$$n! \mathbf{1}\{z_1 < \dots < z_n\} f(z_1) \dots f(z_n).$$

A major characteristic of order statistics is that they allow quantiles approximations. The quantiles are one of the most easy-to-use tools for characterising a probability distribution. In practice, the data distribution can be described by such empirical quantiles.

Two prominent aspects are now presented. The first one shows how to compute empirical quantiles using order statistics. Let us assume that  $F$  is continuous and that there exists a unique solution  $z_q$  to the equation  $F(z) = q$  with  $q \in (0, 1)$ . Clearly,  $z_q$  is the  $q$ -quantile of  $F$ . Let  $(k(n), n \geq 1)$  be an integer sequence with  $1 \leq k(n) \leq n$  and  $\lim_{n \rightarrow \infty} \frac{k(n)}{n} = q$ . Then the sequence of the empirical quantiles  $(Z_{(k(n),n)}, n \geq 1)$  converges almost surely towards  $z_q$ .

The second aspect allows the computation of confidence intervals and hypothesis testing. If  $Z_1$  has a continuous probability

density  $f$  with  $f(z_q) > 0$  for  $q \in (0, 1)$  and if it is supposed that  $k(n) = nq + o(\sqrt{n})$ , then  $Z_{(k(n),n)}$  converges in distribution towards  $z_q$  as follows:

$$\sqrt{n}(Z_{(k(n),n)} - z_q) \xrightarrow{\mathcal{L}} \mathcal{N}\left(0, \frac{q(1-q)}{f(z_q)^2}\right).$$

The exploratory analysis we propose for the perturbation data sets is based on the computation of empirical quantiles. There are several reasons motivating such a choice. First, little is known about the prior distribution concerning the perturbation marks, except that they are distributed around zero and that they are uniformly located in  $K$ . This implies that very few hypotheses with respect to the data can be made. Clearly, in order to apply such an analysis the only assumptions needed are the conditions of validity for the central limit theorem. From a practical point of view, an empirical quantiles-based analysis allows the checking of the tails, the symmetry and the general spatial pattern of the data distribution. From a theoretical point of view, the mathematics behind this tool allow us a rather rigorous analysis.

## 2.3. Stable distribution models

Stable laws are a rich class of probability distributions that allow heavy tails and skewness and have many nice mathematical properties. They are also known in the literature under the name of  $\alpha$ -stable, stable Paretian or Lévy stable distributions. These models were introduced by Levy (1925). Below some basic notions and results on stable distributions are given (Borak et al. 2005; Feller 1971; Samorodnitsky & Taqqu 1994).

A random variable  $Z$  has a *stable distribution* if for any  $A, B > 0$ , there is a  $C > 0$  and  $D \in \mathbb{R}^1$  in a way that

$$AZ_1 + BZ_2 \stackrel{\mathcal{L}}{=} CZ + D,$$

where  $Z_1$  and  $Z_2$  are independent copies of  $Z$ , and “ $\stackrel{\mathcal{L}}{=}$ ” denotes equality in distribution.

A stable distribution is characterised by four parameters  $\alpha \in (0, 2], \beta \in [-1, 1], \gamma \geq 0$  and  $\delta \in \mathbb{R}^1$  and it is denoted by  $\mathcal{S}_\alpha(\beta, \gamma, \delta)$ . The role of each parameter is as follows:  $\alpha$  determines the rate at which the distribution tail converges to zero,  $\beta$  controls the skewness of the distribution, whereas  $\gamma$  and  $\delta$  are the scale and shift parameters, respectively. Figure 1 shows the influence of these parameters on the distribution shape.

The linear transformation of a stable random variable is also a stable variable. If  $\alpha \in (0, 2)$ , then  $\mathbb{E}|Z|^p < \infty$  for any  $0 < p < \alpha$  and  $\mathbb{E}|Z|^p = \infty$  for any  $p \geq \alpha$ . The distribution is Gaussian if  $\alpha = 2$ . The stable variable with  $\alpha < 2$  has an infinite variance, and the corresponding distribution tails are asymptotically equivalent to a Pareto law (Skorokhod 1961). More precisely

$$\begin{cases} \lim_{z \rightarrow \infty} z^\alpha \mathbb{P}\{Z > z\} = \frac{(1+\beta)}{2} \sigma, \\ \lim_{z \rightarrow -\infty} z^\alpha \mathbb{P}\{Z < -z\} = \frac{(1-\beta)}{2} \sigma. \end{cases} \quad (2)$$

where  $\sigma = C_\alpha \gamma^\alpha$ ,  $C_\alpha = \frac{1-\alpha}{2\Gamma(2-\alpha)\cos(\pi\alpha/2)}$  if  $\alpha \neq 1$  and  $C_\alpha = \frac{2}{\pi}$  elsewhere. The distribution is symmetric whenever  $\beta = 0$ , or skewed otherwise. In the case  $\alpha < 1$ , the support of the distribution  $\mathcal{S}_\alpha(\beta, \gamma, 0)$  is the positive half-line when  $\beta = 1$  and the negative half-line when  $\beta = -1$ . If  $\alpha > 1$ , then the first order moment exists and equals the shift parameter  $\delta$ .

One of the technical difficulties in the study of stable distribution is that except for a few cases (Gaussian, Cauchy and

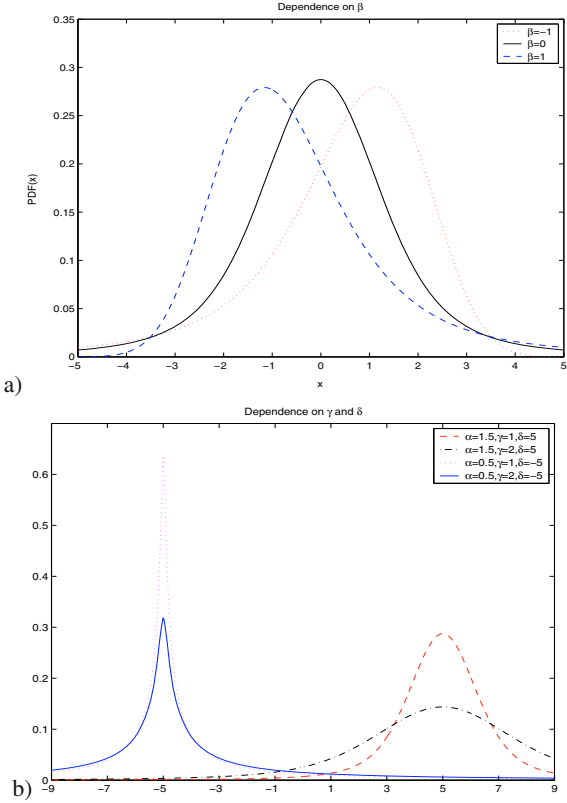


**Fig. 1.** Influence of the parameters on the shape of a stable distribution: **a)**  $\beta$  parameter; **b)**  $\alpha$ ,  $\gamma$  and  $\delta$  parameters.

Lévy), there is no explicit form for the densities. The characteristic function can be used instead to describe the distribution. There exist numerical methods able to approximate the probability density and the cumulative distribution functions (Nolan 1997). Simulation algorithms for sampling stable distribution can be found in Borak et al. (2005); Chambers et al. (1976).

Due to the previous considerations, parameter estimation is still an open and challenging problem. Several methods are available in the literature (Fama & Roll 1971; McCulloch 1986; Mittnik et al. 1999; Nolan 2001; Press 1972). Nevertheless, these methods all have the same drawback in the sense that the data is supposed to be a sample of a stable law. It is a well known fact that if the data come from a different distribution, the inference of the tail index may be strongly misleading. A solution to this problem is to estimate the tail exponent (Hill 1975) and then estimate distribution parameters if  $\alpha \in (0, 2]$ .

Still, there remains the problem of the parameter estimation whenever the tail exponent is greater than 2. Under these circumstances, distributions with regularly varying tails can be considered. A random variable has a distribution with regularly varying tails of an index of  $\alpha \geq 0$  if  $p, q \geq 0, p + q = 1$  and a slowly varying function  $L$ , i.e.  $\lim_{z \rightarrow \infty} \frac{L(\lambda z)}{L(z)} = 1$  for any  $\lambda > 0$ , so that

$$\begin{cases} \lim_{z \rightarrow \infty} z^\alpha L(z) \mathbb{P}\{Z > z\} = p, \\ \lim_{z \rightarrow \infty} z^\alpha L(z) \mathbb{P}\{Z < -z\} = q. \end{cases} \quad (3)$$

It is important to notice that the conditions (2) can be obtained from (3) whenever  $L(z) = 1/\sigma$  and  $p = (1 + \beta)/2$ .

The parameter estimation algorithm proposed by Davydov & Paulauskas (1999, 2004) is constructed under the assumption that the sample distribution has the asymptotic property (2). The algorithm gives three estimated values  $\hat{\alpha}, \hat{\beta}, \hat{\sigma}$ . The  $\hat{\delta}$  can be

computed easily whenever  $\alpha > 1$ , by approximating it using the empirical mean of the samples. This parameter estimation method can be used for stable distribution and in this case,  $\hat{\alpha}$  should indicate positive values lower than 2. At the same time, the strong point of the method is that it can be used for data which do not follow stable distributions. In this case the data distribution is assumed to have regularly varying tails. The weak point of this algorithm is that in this case it does not give indications concerning the body of the distribution. Nevertheless this method allows in both cases a rather complete characterisation of a wide panel of probability distributions. The code implementing the algorithm is available just by simple demand to the authors.

### 3. Results

#### 3.1. Empirical quantiles

The lack of stationarity of the perturbation marks imposes the partitioning of the location space in a finite number of cells. Let us consider such a partition  $K = \cup_{i=1}^n K_i$ . The cells  $K_i$  are disjoint, and they all have the same volume. The size of the volume has to be big enough in order to contain a sufficient number of perturbations. At the same time, the volume has to be small enough to allow for stationarity assumptions for the perturbation marks inside a cell. After several trial and errors, we have opted for a partition made of square cells  $K_i$ , all having the same volume  $0.1 \times 0.1$  AU, so that each cell contains about 1500 perturbations.

We were interested in three questions concerning the perturbation marks distributions. The first two questions are related to the tails and the symmetry of the data distribution. The third question is related to a more delicate problem. It is a well known fact that the perturbation locations follow an uniform distribution in  $K$ . Nevertheless, little is known about the spatial distribution of the perturbation marks, except that they are highly dependent on their corresponding locations. So, the third question to be formulated is the following: do the distributions of the perturbation marks exhibit any pattern depending on the perturbation location?

For this purpose, empirical  $q$ -quantiles were computed in each cell. Most of these values indicate that the perturbation marks are distributed around the origin, while no particular spatial pattern is exhibited in the perturbation location space.

On the other hand, the situation is completely different for extreme  $q$ -values such as 0.01, 0.05, 0.95, 0.99. These quantiles indicate rather important values around the semi-major axis of each planet. In order to check if these values may reveal heavy tail distributions, the difference based indicator  $z_q - \hat{n}_q$  was built. The first term of this indicator represents an empirical  $q$ -quantile. The second term is the theoretical  $q$ -quantile of the normal law with mean and standard deviation given by  $z_{0.50}$  and  $0.5(z_{0.84} - z_{0.16})$ . Hence, for values of  $q$  approaching 1, positive values of the indicator may suggest heavy-tail behaviour for the data. Clearly, this indicator may be used also for quantiles approaching 0. In this case, it is the negative sign that reveals the fatness of the distribution tail.

In Fig. 2 the values obtained for the difference indicator  $z_{0.99} - \hat{n}_{0.99}$  are shown. It can be observed that its rather important values appeared whenever the perturbations are located in the vicinity of a planet orbit. All these values tend to form a spatial pattern similar to an arrow-like shape. As it can be observed, this shape is situated around the planet orbit and points from the right to left. It tends to vanish when the cosine of the inclination angle approaches  $-1$ . The prominence of this arrow shape clearly depends on the closest planet: the bigger the planet, the

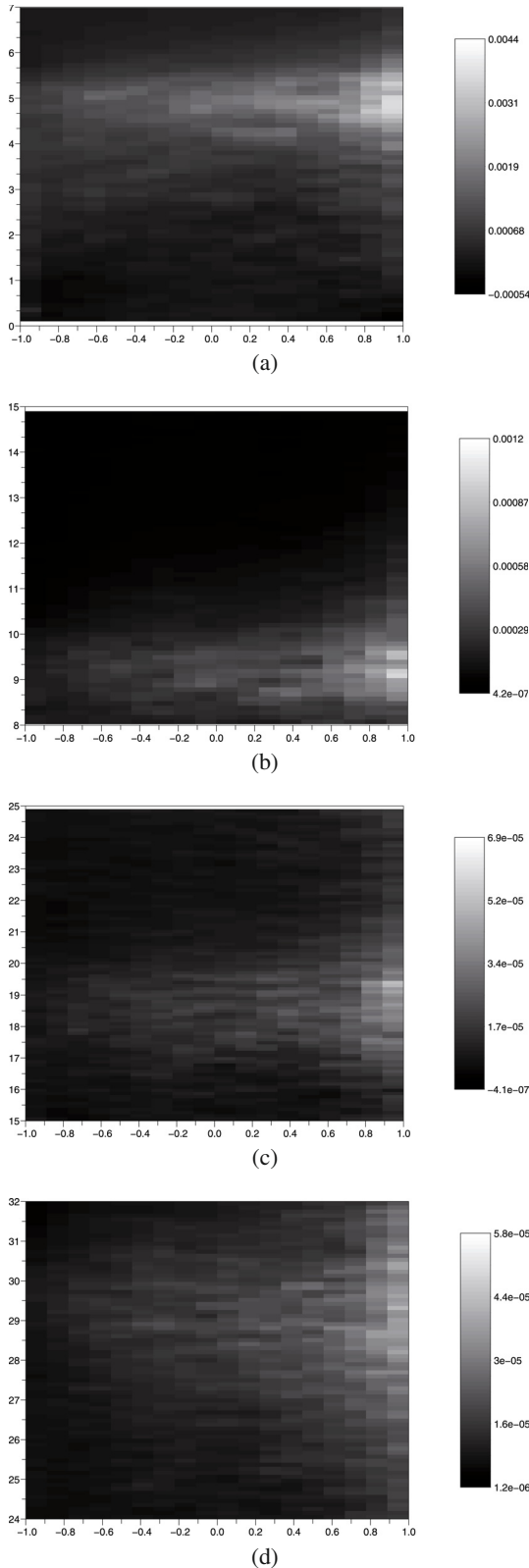


**Fig. 2.** Empirical quantiles based difference indicator  $z_{0.99} - \widehat{n}_{0.99}$  for the perturbation marks around the major planets. The corresponding range intervals are specified in parentheses: **a)** Jupiter ( $[-0.0005, 0.0044]$ ); **b)** Saturn ( $[4.2 \times 10^{-7}, 0.0012]$ ); **c)** Uranus ( $[-4.1 \times 10^{-7}, 6.9 \times 10^{-5}]$ ); and **d)** Neptune ( $[1.2 \times 10^{-6}, 5.8 \times 10^{-5}]$ ). For each diagram the  $y$ -axis corresponds to the initial perihelion distance in AU, and the  $x$ -axis to the cosine of the inclination. We recall that the respective semi-major axis of the four giant planets are  $a_J = 5.2$  AU,  $a_S = 9.6$  AU,  $a_U = 19.2$  AU,  $a_N = 30.1$  AU.

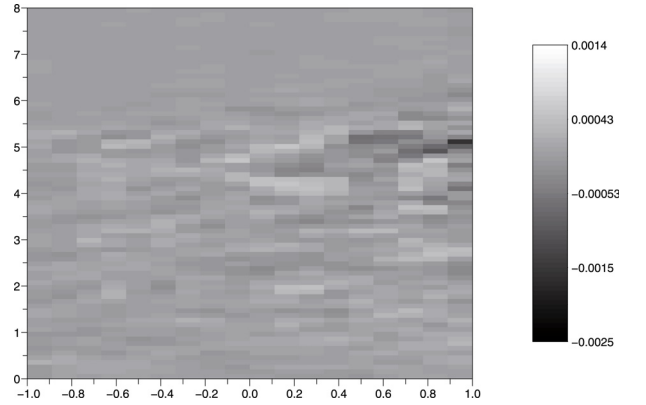


**Fig. 3.** Exploring the symmetry using empirical quantiles difference  $z_{0.99} - |z_{0.01}|$  for the perturbation marks around Jupiter. Axis are as for Fig. 2. The range interval is  $[-0.0025, 0.0014]$ .

sharper is the arrow-like shape. This can be observed by looking at the change of values for the difference indicator with respect to the size of the planet. These observations fulfil some common sense expectations: the comet perturbations tend to be more important whenever a comet crosses the orbit of a giant planet.

Since these phenomena are observed for extremal  $q$ -quantiles, they indicate that the distribution tails may be an important feature for the data. Hence, a statistical model for the data should be able to reproduce these characteristics of the perturbation marks.

Empirical quantiles can be also used in a straightforward way as symmetry indicators of the data distribution. Clearly, by just checking whenever the difference  $z_q - |z_{1-q}|$  tends to 0, this may suggest a rather symmetric data distribution. Figure 3 shows the computation of such differences for each data cell. The values obtained are rather low all over the studied region. Nevertheless, there are some regions, and especially around the Jupiter's orbit we may suspect the data distributions to be a little bit skewed. Still, since the perturbations have comparatively low numerical values, assessing the symmetry using the proposed indicator has to be done cautiously.

It is reasonable to expect a more reliable answer concerning this question by using a statistical model. Clearly, such a model should be able to reproduce the symmetry of the data distribution as well.

The central limit theorem available for the order statistics allows the construction of an hypothesis test. Since our analysis leads us towards heavy-tailed distribution models, a statistical test was performed as a precaution to verify whether a more simple model can be fit to the data. The normality assumption was considered as the null hypothesis for the test. The test was performed for the data in each cell, by considering that the normal distribution parameters are given by the empirical quantiles as explained previously. The  $p$ -values were computed using a  $\chi^2$  distribution. In this context, the local normality assumption for the perturbation marks is globally rejected. Figure 4 shows the result of testing the normality of the  $z_{0.95}$  empirical quantile computed around the Jupiter's orbit.

Indeed, there exist regions where the normality assumptions cannot be rejected for the considered quantile. Still, the regions where this hypothesis is rejected clearly indicate that normality cannot be assumed throughout. Therefore, a parametric statistical model has to be able to reflect this situation and indicate the cases for “heavy” or stable distribution tails.

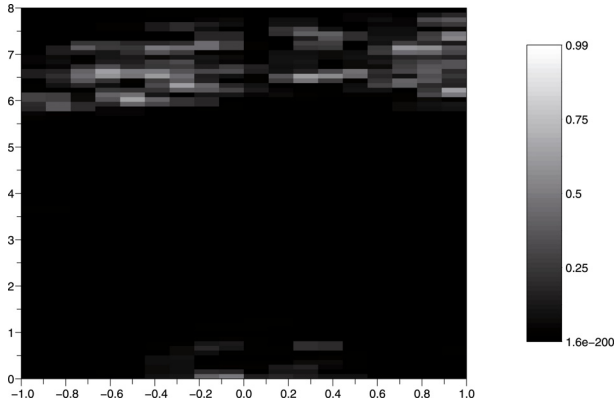


**Fig. 4.**  $p$ -values computed to test the normality of the empirical quantiles  $z_{0.95}$  around Jupiter.

The only parameter used during this exploratory analysis was the partitioning of the location domain  $K$ . There is one more question to answer: do the obtained results depend on the patterns exhibited by the data, or they are just a consequence of the partitioning in cells of the data locations? To answer this question, a bootstrap procedure and a permutation test were implemented (Davison & Hinkley 1997).

Bootstrap samples were randomly selected by uniformly choosing 20% from the entire perturbations data set. Difference indicators were computed for this special data set. This operation was repeated 100 times. At the end of the procedure, the empirical means of the difference indicators were computed. In Fig. 5a the bootstrap mean of the indicator  $z_{0.99} - \widehat{n}_{0.99}$  around Jupiter's orbit is shown. As expected, the same pattern is obtained as in Fig. 2a: important values are grouped around the planet's orbit and exhibit an arrow-like shape pointing from right to left.

The permutation test follows the same steps as the bootstrap procedure except that the perturbations are previously permuted. This means that all the perturbations are modified as follows: for a given perturbation the mark is kept while its location is exchanged with the location of another randomly chosen perturbation. This procedure should destroy any pre-existing structure in the data. In this case, we expect that applying a bootstrap procedure on this new data set will indicate no relevant patterns. In Fig. 5b the result of such a permutation test is shown. The experiment was carried out in the vicinity of Jupiter's orbit. After permuting the perturbations as indicated, the previously described bootstrap procedure was applied in order to estimate bootstrap means of the difference indicator  $z_{0.99} - \widehat{n}_{0.99}$ . The result confirmed our expectations in the sense that no particular structure or pattern is observed. This clearly indicates that the analysis results were due mainly to the original data structure and not to the partitioning of the perturbations location domain in cells.

At the same time, the permutation test is also a verification of the proposed exploratory methodology. This methodology depends on a precision parameter to characterise the hidden structure or pattern exhibited by the data. Still, whenever such a structure does not exist at all, the present method detects nothing.

### 3.2. Inference using heavy-tail distributions

The empirical observations of the perturbation marks distributions indicated fat tails and skewness behaviour. This leptokurtic character of the perturbation distributions was observed especially in the vicinity of the planets' orbits. In response to this empirical evidence heavy-tail distribution modeling was chosen.

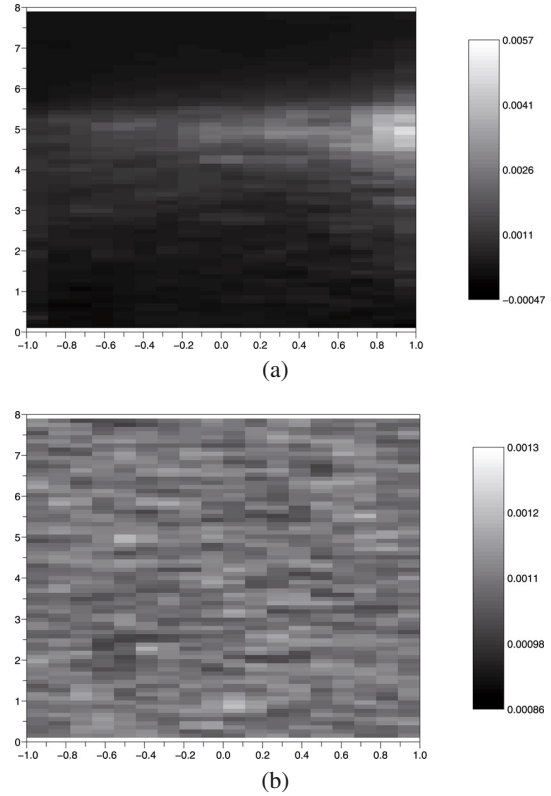


**Fig. 5.** Validation of the analysis based on the computation of the difference indicator  $z_{0.99} - \widehat{n}_{0.99}$  around Jupiter. The corresponding range intervals are given in parentheses: **a)** bootstrap procedure  $([-0.0004, 0.0057])$ ; **b)** permutation test  $([0.0008, 0.0013])$ .

The same cell partitioning as for the exploratory analysis is maintained. The previously mentioned algorithm to estimate stable law parameters was run for the data in each cell.

In Fig. 6 the estimation result of the tail exponent is shown. A region can be clearly observed which is formed by the cells corresponding to estimated  $\alpha$  values lower than 2. This kind of region may be located around each orbit which corresponds to a big planet. The shape of this region is less picked than the region obtained using empirical quantiles. Still, the two results are coherent. Both results indicate that the heavy-tailed character of the perturbations distributions exhibits a spatial pattern. This spatial pattern is located around the orbits of the major planets.

The skewness of the data distribution can be analysed by looking at the results shown in Fig. 7. Indeed, it can be observed that there are cells containing perturbations following a skewed distribution. The obtained results indicate neither the presence of a pattern by such distributions nor the presence of such a pattern around the orbits of the major planets.

The estimation results for the  $\sigma$  and  $\delta$  parameters are presented in Fig. 8. The scale parameter indicates how heavy the distribution tails are. It may be observed in Fig. 8a that the most important values of  $\sigma$  tend to form a spatial pattern similar to the patterns formed by the difference indicator based on order statistics and the tail exponent, respectively. The results obtained for the  $\delta$  parameter indicate that a shift of the perturbation may exist around the orbit of the corresponding big planets.

To check these results a statistical test using the central limit theorem for order statistics was built. This result can be used to verify if the empirical quantiles from a cell are coming from the distribution characterised by the parameters previously

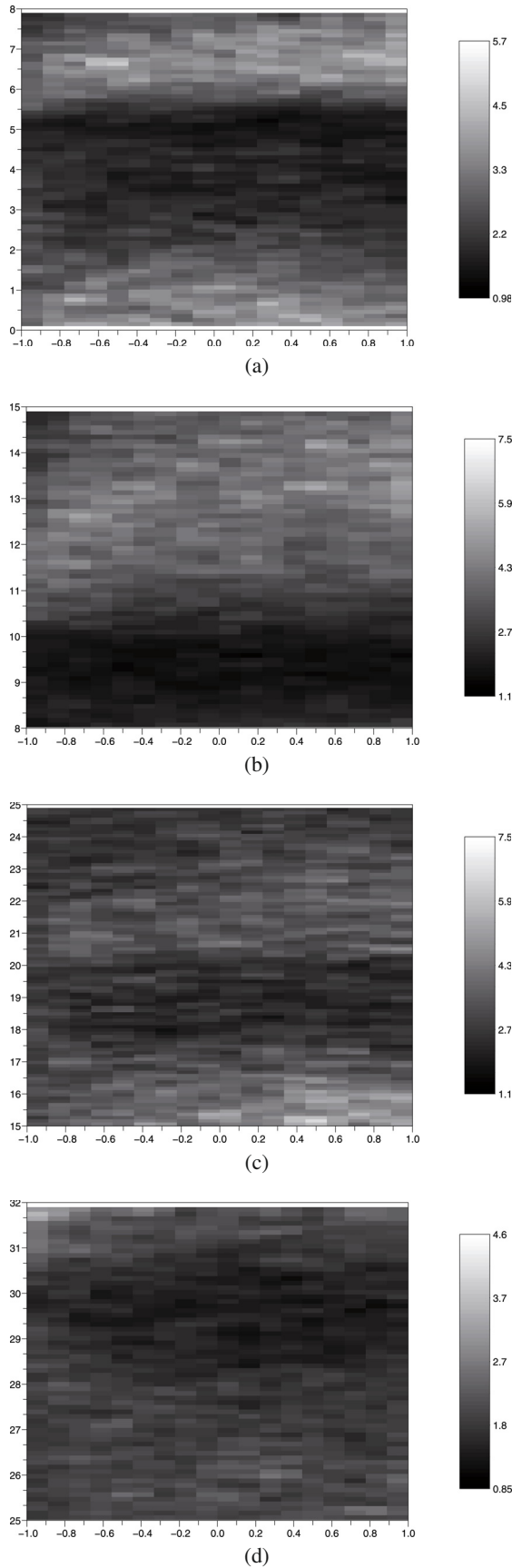


**Fig. 6.** Estimation result of the tail exponent  $\alpha$  for the perturbation marks around the major planets. The corresponding range intervals are given in parentheses: **a)** Jupiter ([0.98, 5.7]); **b)** Saturn ([1.1, 7.5]); **c)** Uranus ([1.1, 7.5]) and **d)** Neptune ([0.85, 4.6]).

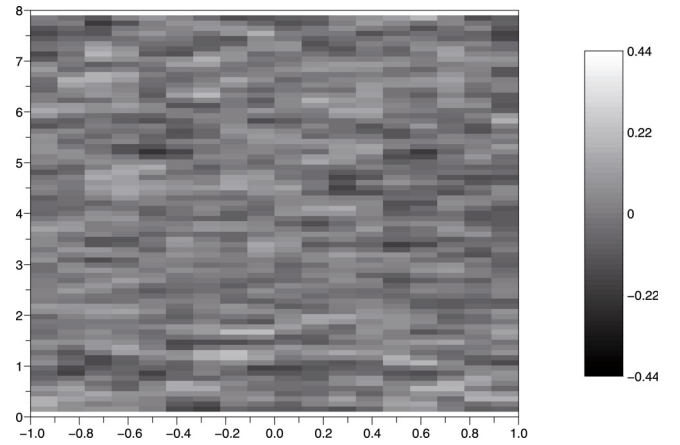


**Fig. 7.** Estimation result of the skewness parameter  $\beta$  for the perturbation marks around Jupiter. The range interval is  $[-0.44, 0.44]$ .

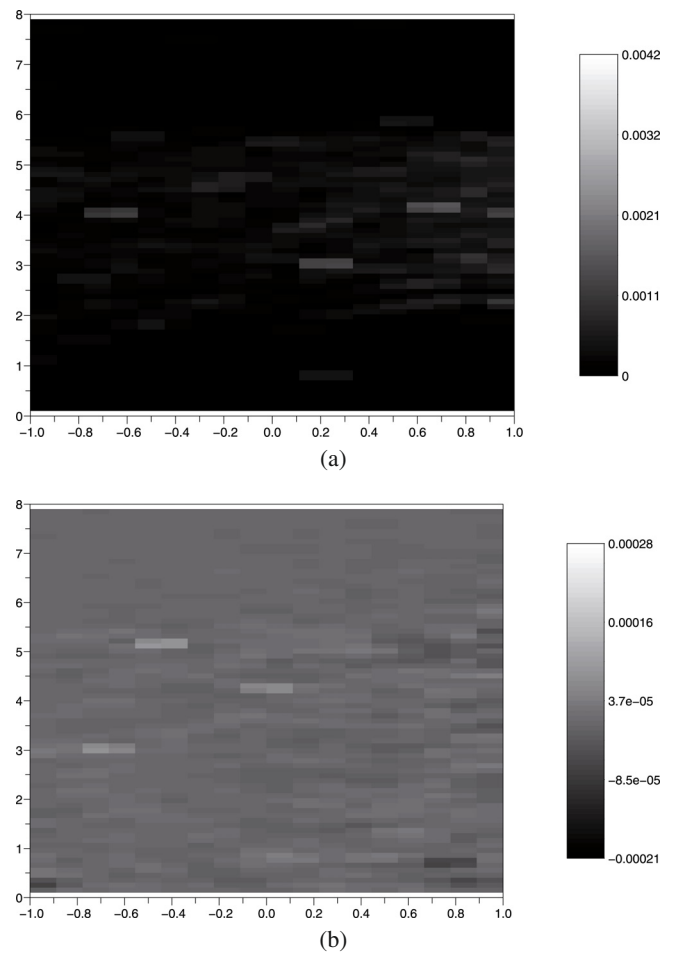


**Fig. 8.** Estimation result of the scale parameter  $\sigma$  range interval  $[0, 0.0042]$  and shift parameter  $\delta$  range interval  $[-0.0002, 0.0002]$  for the perturbation marks around Jupiter.

estimated. Figure 9 shows the result of a test verifying that the  $z_{0.99}$  quantiles around the Jupiter’s orbit are originated from a heavy-tail distribution, while the quantiles outside this region are coming instead from Pareto distribution. It can be observed that high results for the  $p$ -values are spread around the entire region: for 81.5% of the cells we cannot reject the null hypothesis. This result is obviously a far better characterisation of the distribution

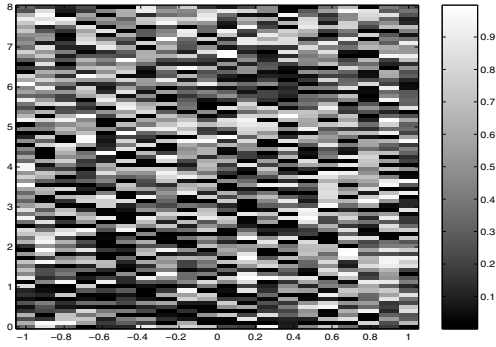


**Fig. 9.**  $p$ -values computed to test if the empirical quantiles  $z_{0,99}$  around the Jupiter's orbit are originated from a heavy-tail distribution.

tails of the perturbations than the test for the normality assumption performed in the preceding section.

The previous test certifies that the perturbations distributions tails exhibit a stable or regular variation behaviour. If the perturbations are close to the orbit of a big planet they have mainly a stable behaviour. Figure 10 shows the  $p$ -values of a  $\chi^2$ -test implemented for the perturbations with an estimated tail exponent  $\alpha < 2$ . This test allows us to check the perturbations also for their distribution body. It can be observed that in almost all these regions the assumption of stable distributions is accepted.

For the perturbations with a tail exponent greater than 2, an alternative family of distributions with regularly varying tails was considered for modelling. Its expressions is given below:

$$f(z) = \frac{C_{\kappa,\alpha}}{1 + |\kappa z - \omega|^{\alpha+1}}, \quad (4)$$

with  $C_{\kappa,\alpha}$  the normalising constant,  $\kappa$  the scale parameter,  $\omega$  the location parameter and  $\alpha$  the tail exponent.

The parameter estimation for such distributions was done in several steps. First, the tail exponent  $\alpha$  was obtained from the previous algorithm. Second, the location parameter  $\omega$  was estimated by the empirical mean of the data samples. Finally, the normalising constant  $C_{\kappa,\alpha}$  and the scale parameter  $\kappa$  were estimated using the method of moments.

A  $\chi^2$  statistical test was done for the perturbations with  $\alpha \geq 2$ . The null hypothesis considered was that the considered perturbations follow a regularly varying tail distribution (4) with parameters given by the previously described procedure. The obtained  $p$ -values are shown in Fig. 11. It can be noticed that in the majority of considered cells the null hypothesis is accepted.

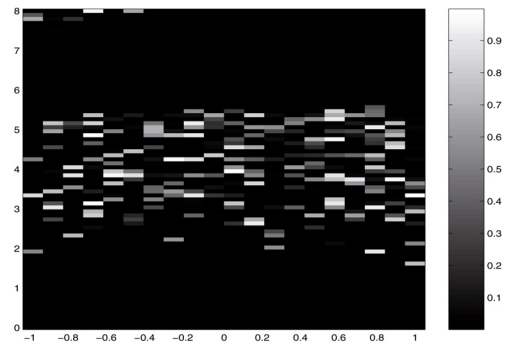
#### 4. Discussion and interpretation

Some of the features present in the Figures can be explained in the framework of the analytical theory of close encounters (Opik 1976; Greenberg et al. 1988; Carusi et al. 1990; Valsecchi & Manara 1997).

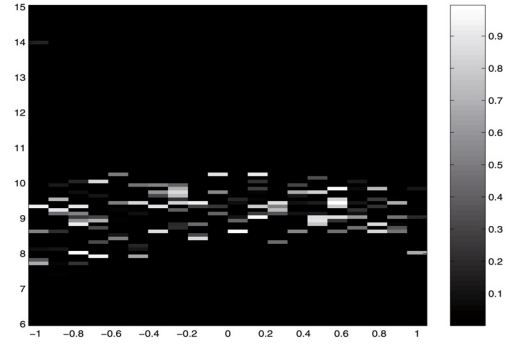
Let us consider the magnitude of the perturbations in the vicinity of  $a = a_j = 5.2$  AU (Jupiter). The colour coding of Fig. 2 is related to the magnitude  $P$  of the perturbation, corresponding to

$$Z = -\frac{1}{a_f} + \frac{1}{a_i} \propto h_f - h_i, \quad (5)$$

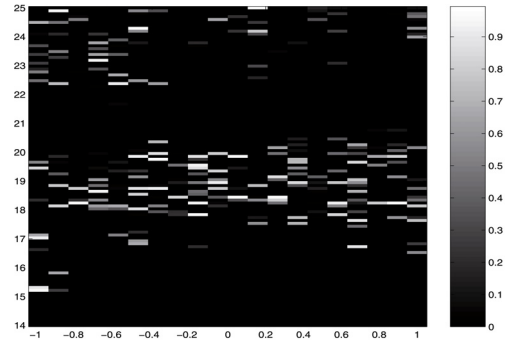
where  $a$  and  $h$  are the orbital semi-major axis and the orbital energy of the heliocentric Keplerian motion of the comet respectively. The subscripts  $i$  and  $f$  stand, respectively, for *initial* and *final*, i.e., before and after the interaction with Jupiter.



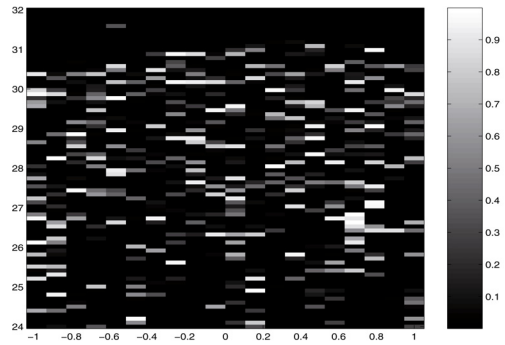
(a)



(b)



(c)



(d)

**Fig. 10.**  $p$ -values of a  $\chi^2$  statistical test for the perturbations with  $\alpha < 2$  around the major planets: **a)** Jupiter; **b)** Saturn; **c)** Uranus; **d)** Neptune.

Perturbations at planetary encounters are characterised by large and in general asymmetric tails, as was shown by various authors (Everhart 1969; Oikawa & Everhart 1979; Froeschlé & Rickman 1981); an analytical explanation of these features was given by Carusi et al. (1990) and by Valsecchi et al. (2000), and



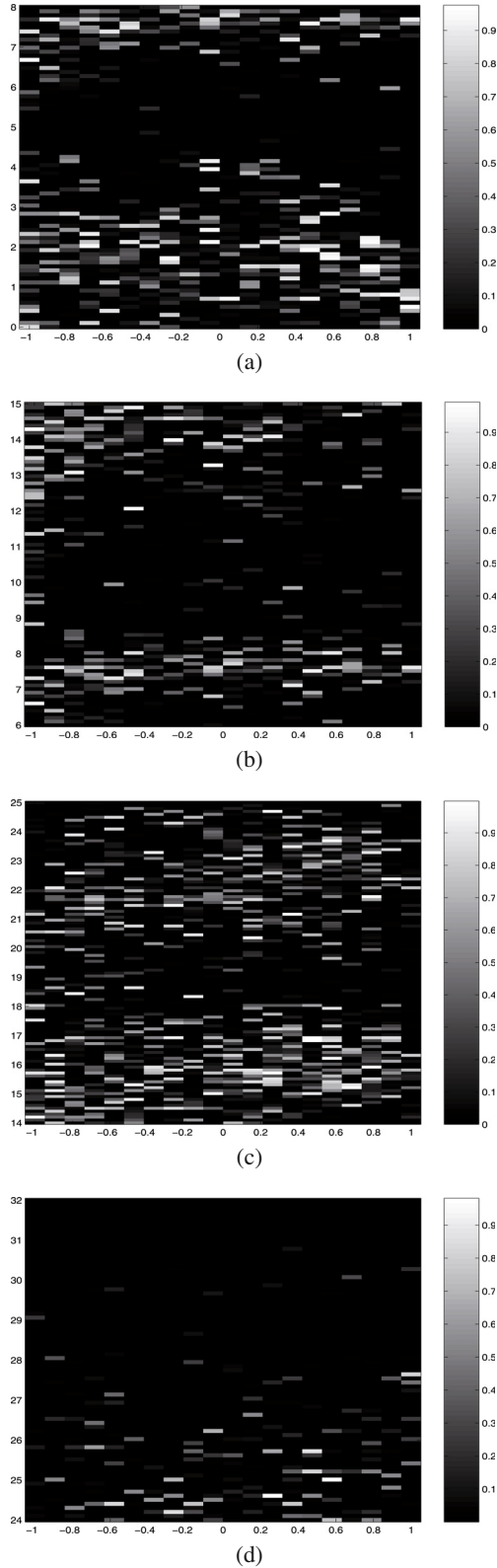


**Fig. 11.**  $p$ -values of a  $\chi^2$  statistical test for the perturbations with  $\alpha \geq 2$  around the major planets: **a)** Jupiter; **b)** Saturn; **c)** Uranus; **d)** Neptune.

the consequences on the orbital evolution of comets was discussed by Valsecchi & Manara (1997).

We now consider the case of parabolic initial orbits (our orbits are in fact very close to parabolic), and discuss the

conditions under which we can expect asymmetric tails in the energy perturbation distributions.

The condition for the tails of the energy perturbation distribution to be symmetric is (Carusi et al. 1990; Valsecchi et al. 2000):

$$\cos \theta = 0,$$

where we have for a parabolic orbit:

$$\begin{aligned} \cos \theta &= \frac{1 - U^2}{2U} \\ U &= \sqrt{3 - 2\sqrt{2q/a_p} \cos i} \\ \cos \theta &= \frac{\sqrt{2q/a_p} \cos i - 1}{\sqrt{3 - 2\sqrt{2q/a_p} \cos i}}, \end{aligned}$$

where  $a_p$  is the orbital semi-major axis of the planet encountered, and  $U$  is the planetocentric velocity of the comet at encounter, in units of the orbital velocity of the planet itself. Making the appropriate substitutions, the condition  $\cos \theta = 0$  in the  $q$ - $\cos i$  plane turns out to be:

$$\cos i = \sqrt{\frac{a_p}{2q}}.$$

Anyway, the finite size of the available perturbation sample must be taken into account, as the tails would become sufficiently populated to show any asymmetry only for very large samples.

Turning our attention now more generally to the tails of the energy perturbation distributions, we consider that in different regions of the  $q$ - $\cos i$  plane the probability  $p$  for the comet on a parabolic orbit to pass within a given unperturbed minimum distance  $b$  from the planet (the so-called *impact parameter*) would be, according to Opik (1976)

$$p(b) = \frac{b^2}{a_p^2 \pi \sin i \sin \theta |\sin \phi|} = \frac{b^2}{a_p^2} \frac{U}{\pi \sin i \sqrt{2 - 2q/a_p}}. \quad (6)$$

We note that  $p(b)$  can also be considered to be the probability with which the comet passes within *any* circle of a given radius  $b$  on the target plane (the plane centred on the planet, and perpendicular to the unperturbed planetocentric velocity of the comet).

As for the size of the perturbation, Valsecchi et al. (2000) show that, in the target plane, the locus of points through which the comet has to pass in order to undergo an energy perturbation

$$z = -\frac{a_p}{a_f} + \frac{a_p}{a_i},$$

(where  $a_i$  and  $a_f$  are the semi-major axes of the orbit before and after the encounter with the planet) is a circle of radius

$$R = \frac{m_p a_p}{m_\odot U^2} \frac{\sin \theta'}{|\cos \theta' - \cos \theta|},$$

where, for a pre-encounter parabolic orbit,  $\cos \theta$  has the expression seen before, while for  $\cos \theta'$  and  $\sin \theta'$ , which refer to the post-encounter orbits that in general are not parabolic, we have

$$\begin{aligned} \cos \theta' &= \frac{1 - U^2 - a_p/a_f}{2U} \\ \sin \theta' &= \frac{\sqrt{2U^2(3 - a_p/a_f) - (1 - a_p/a_f)^2 - U^4}}{2U}; \end{aligned}$$

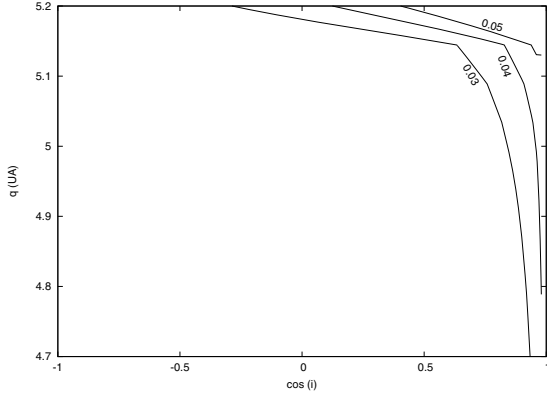


**Fig. 12.** Level curves of  $z_+$  around the semi-major axis of Jupiter. The level of each curve is indicated on the figure.

in our case, in which  $a_p/a_i = 0$  and  $z = -a_p/a_f$ , this radius is:

$$R(z) = \frac{m_p a_p}{m_\odot U^2} \frac{\sqrt{2U^2(3+z) - (1+z)^2 - U^4}}{|z|}.$$

Thus, the probability of an energy perturbation of a size equal or greater than  $z$  is proportional to the surface of the circle of radius  $R(z)$ .

Moreover, as noted above, the probability that a comet passes within a circle of a given radius, say  $R(z)$ , on the target plane can be computed using Öpik's expression (6); we therefore conclude that the probability  $P(z)$  that the comet undergoes an energy perturbation of a size equal or greater than  $z$  is

$$p(z) = \frac{m_p^2}{m_\odot^2} \frac{2U^2(3+z) - (1+z)^2 - U^4}{\pi U^3 z^2 \sin i \sqrt{2-2q/a_p}}. \quad (7)$$

Equation (7) may be inverted to derive the value  $z$  of the energy perturbation for which the probability to have a perturbation greater in absolute value than  $z$  is equal to a given  $p$ . We obtain two solutions,  $z_+$  and  $z_-$ , one for the positive perturbations and one for the negative ones. Each solution is given by

$$z_{\pm} = \frac{U^2 - 1 \pm \sqrt{(1-U^2)^2 - (1+U^4-6U^2)(1+p\alpha)}}{1+p\alpha},$$

with  $\alpha = (\pi U^3 \sin i \sqrt{2-2q/a_p}) \cdot m_\odot^2/m_p^2$  and taking always the upper, resp. lower, sign.

Figure 12 shows the level curves of  $z_+$  for  $p = 0.01$ , which is consistent with Fig. 2. As can be seen, the main features of Fig. 2 are reproduced. The arrow-like shape observed during the statistical study can be now observed on the definition domain imposed by the definition of  $z_+$ . This strengthens our interpretation of the features of Fig. 2 as due to the geometry of close approaches described by the Öpik theory.

## 5. Conclusion and perspectives

In this paper a statistical study of the planetary perturbations on Oort cloud comets was carried out. The exploratory analysis of the perturbation distributions based on order statistics indicated the tail behaviour as a determining feature. Following this idea, parametric inference for heavy-tail distributions was

implemented. The obtained results indicated that the perturbations follow heavy-tail stable distributions which are not always symmetric while tending to form a spatial pattern. This pattern is shaped arrow-like and is situated around the orbits of the major planets. A theoretical study was carried out, and it was observed that this pattern is similar to the theoretical curves derived from the Öpik theory. The perturbations outside this arrow-shaped region were not exhibiting a stable character and they were modelled by a family of distributions with regularly varying tails. In both cases, stable and non-stable distributions, the modelling choices were confirmed by a statistical test.

Clearly, these choices and the estimation parameter estimation procedures can be further improved. Nevertheless, the obtained results give good indications and also good reasons for developing a probabilistic methodology able to simulate such planetary perturbations.

*Acknowledgements.* The authors are grateful to Alain Noullez for very useful comments and remarks. They are also grateful to John J. Matese, the referee of the paper, for his helpful comments. Part of this research was supported by the University of Lille 1 through the financial BQR program.

## References

- Borak, S., Härdle, W., & Weron, R. 2005, in *Statistical tools for finance and insurance*, ed. P. Cizek, W. Härdle, & R. Weron, 21, Springer
- Carusi, A., Valsecchi, G. B., & Greenberg, R. 1990, *Celestial Mechanics and Dynamical Astronomy*, 49, 111
- Chambers, J., Mallows, C., & Stuck, B. 1976, *Journal of the American Statistical Association*, 70, 340
- David, H. A. 1981, *Order statistics* (John Wiley and Sons)
- Davison, A. C., & Hinkley, D. V. 1997, *Bootstrap methods and their application* (Cambridge University Press)
- Davydov, Y., & Paulauskas, V. 1999, *Acta Applicandae Mathematicae*, 58, 107
- Davydov, Y., & Paulauskas, V. 2004, *Fields Institute Communications*, 44, 127
- Delmas, J.-F., & Jourdain, B. 2006, *Mathématiques et Applications (SMAI)*, 57, *Modèles aléatoires. Application aux sciences de l'ingénieur et du vivant* (Springer)
- Everhart, E. 1969, *AJ*, 74, 735
- Everhart, E. 1985, in *Dynamics of Comets: Their Origin and Evolution*, ed. A. Carusi & G. B. Valsecchi, *ASSL*, 115, IAU Colloq. 83:185
- Fama, E., & Roll, R. 1971, *Journal of the American Statistical Association*, 66, 331
- Feller, W. 1971, *An introduction to probability theory and its applications – II* (Wiley)
- Fernández, J. 1981, *A&A*, 96, 26
- Fouchard, M., Froeschlé, C., & Valsecchi, G. B. 2003, *MNRAS*, 344, 1283
- Froeschlé, C., & Rickman, H. 1981, *Icarus*, 46, 400
- Greenberg, R., Carusi, A., & Valsecchi, G. B. 1988, *Icarus*, 75, 1
- Hill, B. M. 1975, *Annals of Statistics*, 3, 1163
- Levy, P. 1925, *Calcul des probabilités* (Gauthier Villars)
- McCulloch, J. H. 1986, *Communications in Statistics – Simulation and Computation*, 15, 1109
- Mittnik, S., Doganoglu, T., & Chenyao, D. 1999, *Mathematical and Computer Modelling*, 29, 235
- Nolan, J. P. 1997, *Communications in Statistics – Stochastic Models*, 13, 759
- Nolan, J. P. 2001, in *Lévy Processes*
- Oikawa, S., & Everhart, E. 1979, *AJ*, 84, 134
- Opik, E. J. 1976, *Interplanetary encounters: close-range gravitational interactions*, ed. E. J. Opik
- Press, S. J. 1972, *Journal of the American Statistical Association*, 67, 842
- Rickman, H., Valsecchi, G. B., & Froeschlé, C. 2001, *MNRAS*, 325, 1303
- Samorodnitsky, G., & Taquq, M. S. 1994, *Stable non-Gaussian random processes: stochastic models with infinite variance* (Chapman & Hall/CRC)
- Skorokhod, A. 1961, in *Selected Translations in Mathematical Statistics and Probability* 1, 157
- Valsecchi, A., & Manara, G. B. 1997, *A&A*, 323, 986
- Valsecchi, G. B., Milani, A., Gronchi, G. F., et al. 2000, *Celestial Mechanics and Dynamical Astronomy*, 78, 83